Chemical Engineering Science 66 (2011) 3358–3368

Contents lists available at ScienceDirect

Chemical Engineering Science

journal homepage: www.elsevier.com/locate/ces

Heat transfer in trickle bed column with constant and modulated feed temperature: Experiments and modeling

N. Habtu [a], J. Font [a], A. Fortuny [a], C. Bengoa [a], A. Fabregat [a], P. Haure [b], A. Ayude [b], F. Stüber [a,*]

[a] Departament d'Enginyeria Química, ETSEQ, Universitat Rovira i Virgili, Paisos Catalanns 26, 43007 Tarragona, Catalonia, Spain
[b] INTEMA, CONICET, UNMDP, J.B. Justo 4302, 7600 Mar del Plata, Argentina

ARTICLE INFO

Article history:
Received 1 October 2010
Received in revised form
19 December 2010
Accepted 11 January 2011
Available online 18 January 2011

Keywords:
Trickle bed
Heat transfer
Axial temperature profiles
Wall heat transfer coefficient
Temperature feed modulation
Dynamic Modeling

ABSTRACT

Heat transfer was investigated in an insulated packed bed column with co-current downflow of gas and liquid under constant and periodically modulated gas–liquid feed temperature. Bed temperatures at three axial positions were assessed at steady state for different insulating systems, different gas and liquid flow rates and system pressure. The experimental profiles recorded were modeled with a dynamic pseudo-homogeneous one parameter model to analyze the effect of operating conditions and to deduce coefficients of overall (U) and bed to wall (h_W) heat transfer. It appears that the heat transfer is strongly affected by the system pressure, whereas the liquid flow rate has a smaller influence. The experimental data of h_W were correlated with the operating conditions leading to a small average error of 7% in the correlation. Condensation of water vapor occurring in the column seems to contribute to the heat transfer inside the packed bed. Several dynamic experiments modulating the feed temperature were also conducted and described with the help of the dynamic model. Predictions with the fitted values of U were in good agreement with experiments and give confidence to apply this model in the investigation of the catalytic wet air oxidation of phenol over carbon conducted in a trickle bed reactor under temperature feed modulation.

1. Introduction

Trickle bed reactors (TBRs) are multiphase systems consisting of a packed bed of catalyst with co-current downflow of gas and liquid. They are used extensively for hydrotreating and hydrodesulfurization applications in the refining industry and for hydrogenation, oxidation and hydrodenitrogenation applications in the chemical, biochemical and waste treatment industry (Khadilkhar et al., 1999). The performance of TBRs depends among other factors on the hydrodynamic regime, wetting efficiency, mass transfer between the phases and radial and axial temperature distribution within the bed. Thus, designing, optimizing and modeling the operation of TBRs is an established challenge in the field of catalytic reactor engineering.

In the last 40 years, numerous works on TBRs appeared in the literature (Dudukovic et al., 2002), providing useful information on flow regimes, hydrodynamics and mass transfer. Contrary, only a few studies have contributed to the description of heat transfer in TBRs (Lamine et al., 1996). Several correlations of effective bed conductivity and bed to wall heat transfer coefficients (h_W) have been proposed, but deviations of 30–40% were reported when using the empirical correlations of different authors for the prediction of h_W (Babu and Sastry, 1999). A further obstacle for their application is that most of these heat transfer studies have been carried out with the classical water-air-inert packing system at ambient conditions of temperature and pressure. Hence, values of heat transfer coefficients may not be representative of actual industrial reactors.

Most TBRs operate with continuous liquid and gas flows but there is evidence that performance enhancement in terms of production, selectivity and/or improved catalyst stability is feasible if the reactor operates at unsteady-state or periodic conditions. The term 'periodic operation' refers to an operation, in which one or more chemical reactor parameters (feed flow rates, composition or temperatures) are periodically varied in time (Silveston and Hanika, 2002).

Employing this process intensification strategy, Gabbiye et al. (2009) reported promising preliminary results on phenol oxidation over activated carbon carried out in a TBR with modulated feed temperature. With this approach, adsorption-reaction cycles are imposed on reactor operation and the performance of an insulated TBR is improved in terms of catalyst stability. To explain these outcomes with the help of a dynamic reactor model, an accurate estimation of the overall heat transfer coefficient at operating conditions is previously required. Moreover, to our knowledge, heat transfer in modulation of feed temperature has not been investigated yet.

* Corresponding author. Tel.: +34 977 559671; fax: +34 977 559621.
E-mail address: frankerich.stuber@urv.cat (F. Stüber).

0009-2509/$ - see front matter © 2011 Elsevier Ltd. All rights reserved.
doi:10.1016/j.ces.2011.01.032

In this contribution, we studied thus the heat transfer of a thermally insulated packed bed of active carbon operated with constant and modulated feed temperature. The aim of this study is to highlight the effect of physical operating variables (total pressure, gas and liquid flow rates, characteristics of insulating material) on heat transfer at steady state conditions. A (dynamic) pseudo-homogeneous one parameter model is formulated and solved to examine the thermal profiles obtained in the packed bed and to estimate coefficients of overall and bed to wall heat transfer. This data are then used in the dynamic model to simulate the experiments conducted with a TBR under modulation of feed temperature but in absence of reaction. The ultimate aim of this nonreactive model developed will be its implementation in a complete reaction–adsorption model that is conceived to simulate a periodically operated trickle bed reactor applied to the CWAO of phenol (Gabbiye et al., 2009).

2. Experimental

2.1. Materials

Deionized water and high purity compressed synthetic nitrogen were used in the experiments. A wood based activated carbon (Merck ref. #102518, $V_{pore}=0.55\ cm^3\ g^{-1}$) was employed as packing material. Prior to TBR experiments, the activated carbon provided in form of 2.5 mm particles was crushed and sieved (25–50 mesh) to obtain the mean diameter fraction of 0.5 mm. Each active carbon sample was rinsed to remove fines, dried at 105 °C overnight, and finally stored under inert atmosphere at 20 °C.

2.2. Experimental set-up

All steady state and dynamic experiments were conducted in a small scale fixed bed column with co-current downflow of gas and liquid. The setup shown in Fig. 1 consists of four zones: (1) an inlet section including water feed and gas feed reservoirs with respective supply lines, (2) a mixing and pre-heating zone, (3) a thermally insulated fixed bed SS-316 column (25 cm long, 0.93 cm DI) and (4) a sequence of sampling device, gas–liquid separator, needle valve and gas flow meter all located at the column outlet. Pure water was transported to the column by a high-pressure metric pump that can dispense flow rates between 0.01 and 0.15 L/h. Liquid flow rates were measured with a water calibrated mass flow meter installed in the liquid line after the liquid dampers. Nitrogen gas was supplied from a high pressure gas cylinder at the required operating pressure with the help of a pressure reducing valve. Gas and liquid phases were mixed by joining the gas and liquid feed lines ca. 2–3 m upstream of the reactor inlet. Before entering the trickle bed at the top of the column, the gas–liquid stream was forced to flow through a metal grid (grid openings <0.1 mm), which acts as a distributor of the gas–liquid mixture. Right after the mixing intersection of gas and liquid lines, a timer controlled three-way valve was placed to enable continuous feeding of hot gas–liquid flow (pre-heated in a 1 m long coil) to the column or alternating cold with hot gas–liquid flow during column operation under feed temperature modulation. The column was carefully filled portion by portion with 7.5 g of activated carbon (AC) to ensure repeatable and uniform packing of particles. The column was further equipped with three thermocouples (with a precision of ± 0.5 K) at axial distances from the inlet of 1.5, 10 and 20.5 cm, respectively, to assess axial temperature profiles during experiments.

Prior to starting the experiments, the system was checked for leaks at ambient temperature and a total pressure of 25 bar; the column was then covered with the type and geometry of insulating material selected for the experiment. Moreover, for minimization of axial heat conduction through the column walls and fitting connections, a system of two flanges with thermal insulation in between has been mounted at the column outlet. Tubing from the pre-heater outlet to the column inlet and from the column outlet to the gas–liquid separator was also insulated in particular to reduce heat loss in the inlet section of the column. After trickling through the packed bed retained by two metal grids, the exited gas–liquid flow was separated and the liquid fraction was stored in the 5 L gas–liquid separator. The residual gas flowing out of the

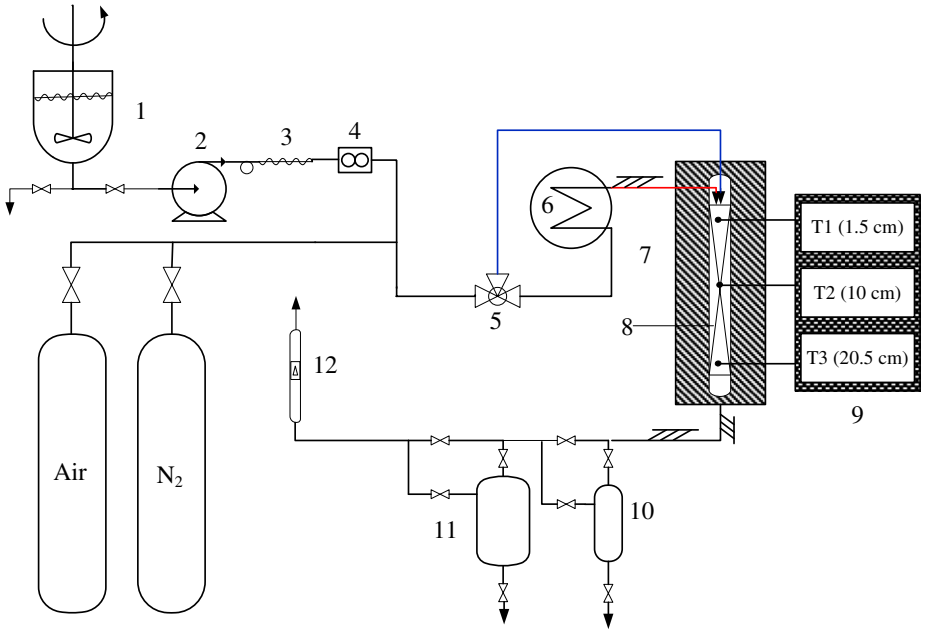

Fig. 1. Experimental set-up for feed temperature modulation: (1) feed, (2) HPL pump, (3) pulse dampener, (4) flow meter, (5) three-way valve (6) heater, (7) insulation material, (8) reactor with flange, (9) temperature display, (10) sampling tube, (11) G–L separator and (12) gas flow meter.

separator was depressurized by means of a needle valve and vented through an air calibrated gas flow meter to measure its volumetric flow rate at ambient pressure and temperature.

To guarantee reproducibility of experimental series, initial conditioning of the trickle-bed has been done following the same protocol. During the start-up, the trickle-bed was contacted with water for ca. 20 min at the highest liquid flow rate of 100 ml/h before feeding the nitrogen at the given flow rate.

2.3. Experiments with constant and modulated feed temperature

All experiments were conducted at low liquid (0.15–1.0) and gas (0.35–4.5) Reynolds numbers, which are typical for trickle-bed reactor studies at laboratory-scale. The final aim of this work is to provide heat transfer data useful for the modeling of phenol CWAO over active carbon carried out in a trickle bed reactor under periodic temperature modulation of gas–liquid feed flow. Hence, two different operation modes were investigated, i.e. experiments with constant feed temperature or periodic change in feed temperature. Table 1 summarizes the operating conditions employed in the experimental series of this work.

Firstly, several insulating materials and geometries were tested to establish axial temperature profiles in the column for the determination of heat transfer parameters under steady state conditions. The following configurations were available in our laboratory: (I) no insulation, (II) two joint rectangular boards of dense ceramic fiber ($10\times2.5\times40\ cm^3$, $\lambda=0.09$ W/m/K), (III) a flexible cylindrical glass fiber wool mantle covered with aluminum foil (O.D.$=5$ cm, $\lambda=0.04$–0.05 W/m/K) and (IV) two joint half cylinders of rock wool foam supported by PVC (O.D.$=11$ cm, $\lambda=0.035$–0.045 W/m/K). The tests were conducted at the following conditions: oven temperature of 170 °C, 16 bar of total pressure, water and nitrogen flow rates of, respectively, 100 ml/h and 18 N L/h using active carbon as packing material of the column.

A few experiments were undertaken with insulating configuration (II) providing the column outlet with a system of two assembled flanges. The aim was to disrupt the axial heat flow through the outlet fittings of the column. To this end, all possible contact points between the two flanges (screws, nuts and flanges itself) were thermally insulated using seals with a low thermal heat conductivity. Experiments conducted with and without flanges at otherwise same operating conditions revealed no differences in axial profiles indicating that the heat loss due to axial wall conduction should not be relevant in our system.

With the insulating system (IV), the effect of operating variables (P_T, F_L and F_G) on the heat transfer in the column was investigated at steady state conditions. In a standard experiment, a liquid flow rate of 100 ml/h was fixed for a given total pressure and gas flow rate to warm up the reactor until reaching stable temperatures. Subsequently, the liquid flow rate was decreased to 60 ml/h to establish a new steady state and then to 30 ml/h. Fig. 2 exemplarily illustrates the temporal evolution of the temperatures recorded in such a standard experiment. The temperatures inside the bed follow with a certain delay the oven temperature.

Table 1
Experimental conditions employed.

Variable	Range	Variable	Range
DI (cm)	0.93	T_{oven} (°C)	170–175
L_R (cm)	25	F_L (ml/h)	30–100
d_P (mm)	0.5	Re'_L	0.16–1.0
ε_B	0.47	F_G (N L/h)	3–18
P_T (bar)	9–25	Re'_G	0.35–4.5

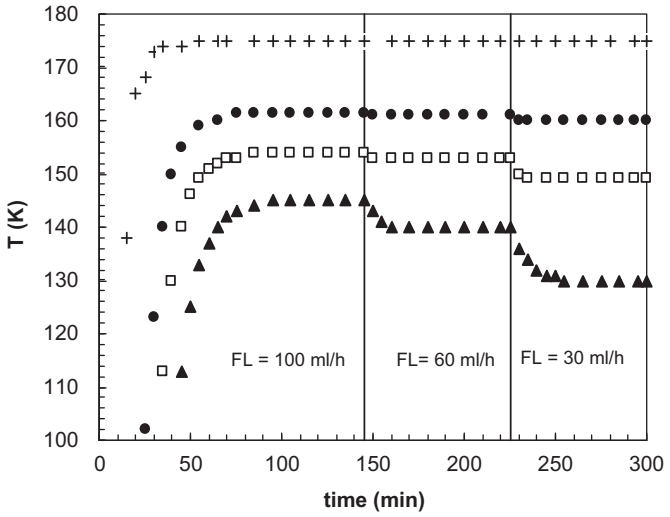

Fig. 2. Evolution of axial temperature during a standard experiment: $P_T=15$ bar, $F_G=9$ N L/h, (+) oven temperature, (●) axial temperature at $z=1.5$ cm, (□) axial temperature at $z=10$ cm, (▲) axial temperature at $z=20.5$ cm.

The difference of 10–15 K between the oven and the column inlet temperatures is essentially due to a worse insulation of the tubing section between the oven outlet and the column inlet. Nevertheless, the initial steady state establishes after ca. 100 min for a liquid flow rate of 100 ml/h. For a subsequent decrease in the liquid flow rate to 60 ml/h and 30 ml/h, it took, respectively, 15 and 30 min to reach stable temperatures (see Fig. 2).

The standard procedure was repeated for different pressures (9–25 bar) and gas flow rates (3–18 N L/h). For each conditions selected, an axial temperature profile was assessed at steady state for posterior determination of the overall and bed to wall heat transfer coefficient by fitting the experimental data to predictions of a pseudo-homogeneous one parameter heat transfer model as described in Section 3. Attention was also paid to the reproducibility of experiments. Several repetition of a standard experiment normally resulted in same axial temperature profiles. Deviations were only observed after dismantling the insulating material of the column and the inlet and outlet lines. In this case, the insulating material was dismantle and properly fixed as to obtain acceptable reproducibility in the temperature profiles. In fact, to avoid this problem a maximum of experiments were done without dismantling the column.

For experiments with feed temperature modulation, the same start-up procedure as for continuous operation was employed. Temperature cycling was started via the timer controlled three-way valve on reaching stable axial temperatures at standard conditions. Dynamic profiles were then assessed during at least two consecutive cycles by recording at regular time intervals of 3–6 min the temperature displayed by each of the three thermocouples mounted along the column. The range of operating parameters studied was limited to conditions that are of particular interest for periodically operated CWAO of phenol: a cycle period of ca. 2 h and a split between 0.8 and 0.9; water and nitrogen flow rates and total system pressure of 0.03–0.1 L/h, 9 N L/h and 10 or 16 bar, respectively.

3. Modeling of trickle-bed heat transfer without reaction

3.1. Pseudo-homogeneous one parameter plug flow model

In the absence of any chemical reaction, no significant interfacial temperature gradients will develop in the trickle-bed and

the use of a pseudo-homogeneous one parameter plug flow model for heat transfer description is reasonable. Moreover, only very flat temperature gradients should establish in radial direction given the particular geometry of our laboratory trickle-bed set-up: insulated narrow tube (0.93 cm in diameter) containing pre-wetted small carbon particles (0.5 mm) acting as acceptable heat conductor. Thus, the model contemplates only one resistance to heat transfer inside the tube, i.e. from the trickle-bed to the inner tube wall at the vicinity of tube wall.

On the other hand, for small tube diameters, wall (flow) effects may become too influent and invalidate the plug flow assumption. However, the validity of plug flow appears to depend on the aspect ratio d_R/d_p rather than on d_R alone. Mariani et al. (2001) concluded in their work that wall effects can be neglected as long as the aspect ratio is >17. The aspect ratio of our trickle-bed takes thus an adequate value of 19 due to the reduced size of the carbon particles. As to axial dispersion of heat, Mears (1971) as cited in a review on criteria to ensure ideal behaviors in trickle-bed reactors (Mederos et al., 2009) established that axial dispersion of heat can be neglected for tube length to particle diameter ratio >30 being as high as 500 in our case.

A last concern is related to the occurrence of liquid maldistribution at small liquid flow rates. To reduce undesired liquid maldistribution, both a narrow tube and small particles are required (the bed itself will then act as a gas–liquid distributor). The importance of particle and tube diameter for flow homogeneity is also reflected in the criteria available in the review of Mederos et al. (2009) for the estimation of liquid maldistribution ($L_R > 0.25 d_R^2/d_p^{0.5}$) and adequate wetting or even irrigation ($W=\mu_L u_L/(\rho_L d_p^2 g) > 4\times 10^{-6}$). Accordingly, the verification of these criteria at the conditions of our study shows that both are fully met by at least one order of magnitude.

Summarizing the heat transfer in our laboratory trickle-bed was modeled based on:

- spherical and isothermal pellets,
- complete internally wetted particle,
- homogeneously packed bed (constant bed porosity),
- negligible pressure drop,
- no thermal gradients between gas, liquid and solid phases,
- no radial thermal gradients and heat dispersion ($d_R/d_p \approx 20$) and no axial heat dispersion ($L_R/d_p \approx 500$),
- heat transfer between packed bed and reactor wall,
- negligible heat loss due to axial conduction,
- instantaneous saturation of gas phase with water vapor.

The non-steady state pseudo-homogeneous energy balance in bulk fluid phase at bed length scale gives then

$$\frac{\partial T}{\partial t} = \frac{-(u_L c_{pL}\rho_L + u_G c_{pG}\rho_G)(\partial T/\partial z) - (\partial \alpha_w^G/\partial z)(\Delta H^V/(\pi(\mathrm{DI}/2)^2)) - U(4/\mathrm{DI})(T-T_{ext})}{(\varepsilon_L c_{pL}\rho_L + \varepsilon_G c_{pG}\rho_G + (1-\varepsilon_L-\varepsilon_G)\varepsilon_P c_{pL}\rho_L + (1-\varepsilon_L-\varepsilon_G)(1-\varepsilon_P)c_{pS}\rho_S)} \tag{1}$$

where

$$\frac{\partial \alpha_w^G}{\partial z} = \frac{(\alpha_T^G)(\partial P_w^v/\partial T)(\partial T/\partial z)}{P_T - P_w^v} = \frac{\left(\alpha_{N_2}^G + ((\alpha_{N_2}^G P_w^v)/(P_T - P_w^v))\right)(\partial P_w^v/\partial T)(\partial T/\partial z)}{P_T - P_w^v}$$

The axial variation of the gas and liquid superficial velocity was calculated as follows:

$$\frac{\partial u_L}{\partial z} = \frac{M_w}{\rho_L \pi(\mathrm{DI}/2)^2}\frac{\partial \alpha_w^L}{\partial z} + \frac{\alpha_w^L M_w}{\pi(\mathrm{DI}/2)^2}\frac{\partial(1/\rho_L)}{\partial z} \tag{2}$$

$$\frac{\partial u_G}{\partial z} = \frac{R_g}{P_T \pi(\mathrm{DI}/2)^2}\left[\frac{T\partial \alpha_w^L}{\partial z} + \left(\alpha_{N_2}^G + \alpha_{N_2}^G \frac{P_w^v}{P_T - P_w^v}\right)\right]\frac{\partial T}{\partial z} \tag{3}$$

The inlet boundary conditions at bed scale are as follows:

$$z=0 \quad T=T_0(t) \quad u_L = u_{L,0} \quad u_G = u_{G,0}$$

3.2. Numerical solution and model parameters

For numerical resolution, the resulting continuous differential equations were all replaced by their finite difference approximations. Solutions to the heat balance in the bulk liquid were obtained with the help of explicit finite differences. A FORTRAN code was developed for the unsteady state model and various discretization strategies were tested to verify model convergence. The dynamic model was solved considering the operating conditions listed in Table 1 and variation of physical properties of gas, liquid and solid phases with temperature. Static and dynamic liquid holdups were evaluated using the correlation proposed by Lange et al. (2005) for low liquid and gas Reynolds numbers.

3.3. Determination of overall (U) and bed to wall heat transfer coefficient (h_W)

For an insulated cylindrical packed bed column with co-current gas–liquid flow, the overall radial heat transfer coefficient U accounts for several radial thermal resistances in series and can be expressed as follows (U is based on the column inside area, R_1):

$$U = \frac{1}{(1/h_W) + ((\ln((R_{IN})/R_1)R_2)/k_{IN}) + ((R_1/(R_{IN}))/h_{NAT})} \tag{4}$$

where h_W represents the bed to wall heat transfer, k_{IN} the thermal conductivity of the insulating material wrapped around the column and h_{NAT} the coefficient of heat transfer due to natural convection between the insulating wall and the surrounding air. Values of h_{NAT} were calculated using the correlation proposed by Churchill and Chu (1975) for laminar flow.

In a first step, the overall heat transfer coefficient U was evaluated for each experiment by searching the value of U that best fits the predicted to the experimental axial temperature profile at steady state. From Eq. (4) and experiments done with and without heat insulation at otherwise same operating conditions, it was also possible to deduce the thermal conductivity of the different insulating materials tested.

The corresponding bed to wall heat transfer coefficients (h_W) were subsequently evaluated from Eq. (4) using the known values of U, k_{IN} and h_{NAT}. Given the values of the thermal conductivity of the insulating material (IV) (0.35 W/(m^2 K) from experiments, 0.35–0.45 W/(m^2 K) from manufacturer), the bed to wall heat coefficients were determined with different k_{IN} ranging from 0.35 to 0.45 W/(m^2 K).

4. Results and discussion

4.1. Effect of insulating material

Fig. 3 shows the axial temperature profiles that establish for the different heat insulating materials tested. As expected, significant heat losses occurred without thermal insulation of the column leading to a bed gradient of ca. -2 K/cm. Accordingly, improvement was found in case of the insulated column, the cylindrical rock wool foam configuration revealing better insulating properties, i.e. a 5 times smaller bed gradient of -0.36 K/cm. Adiabatic conditions were not accomplished as it is desirable to perform experiments with temperature feed modulation. It is noteworthy to state that the experimental axial profiles exhibit a

convex curving as the bed temperature gradient increases. A stronger gradient favors condensation of water vapor from the saturated gas phase and condensation effects may be at the origin of the observed trend.

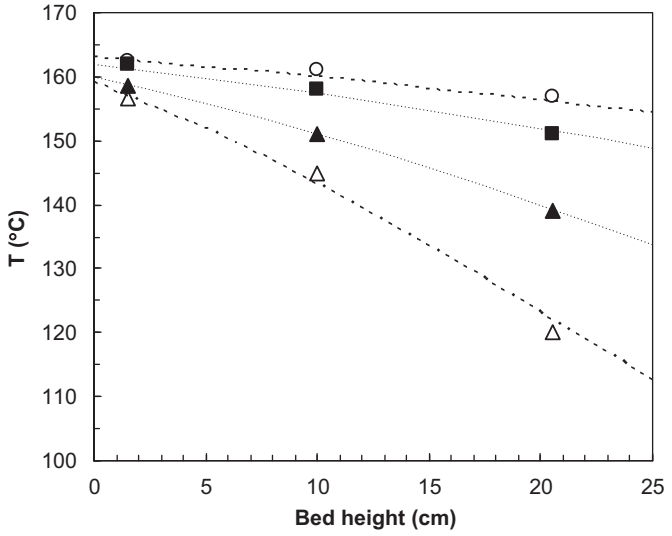

Fig. 3. Influence of different insulating materials and geometries on axial temperature profile in trickle bed column: P_T=15 bar, F_L=100 ml/h, F_G=18 N L/h; (Δ) without isolation, (▲) ceramic fiber, (■) glass fiber, (○) rock wool foam, discontinuous lines represent model predictions.

Fig. 3 also confirms the good match achieved between experimental axial temperature profiles and those predicted from Eq. (1). Further evidence for the overall quality of the experiments and the fitting of the overall heat transfer coefficient U are the thermal conductivities of the insulating materials deduced from Eq. (4), which fall within the range of values extracted from literature or manufacturer data sheets.

4.2. Axial temperature profiles

Representative axial temperature profiles and corresponding steady state predictions are depicted in Fig. 4(a)–(c) for total pressures of 9, 15 and 25 bar, respectively, the 3 liquid flow rates studied and a gas flow rate of 9 N L/h.

Fig. 4 evidences again that the predicted temperature profiles match well the experimental data and this holds for all other experimental conditions tested. A second observation to point out is the strong influence that has pressure on the shape of the temperature profiles. The flat and straight profiles that establish at 9 bar become more steep and curved for intermediate pressure of 15 bar and decreasing liquid flow rate. A further increase to 25 bar results in even steeper profiles, which however show no longer convex curving. The curving of the profiles with pressure may be related to condensation effects as already suggested in Section 4.1. At a total system pressure of 9 bar and 160 °C, the saturated nitrogen phase flowing through the fixed bed contains actually a high fraction (ca. 70%) of water vapor. However, the axial temperature gradients establishing at this pressure

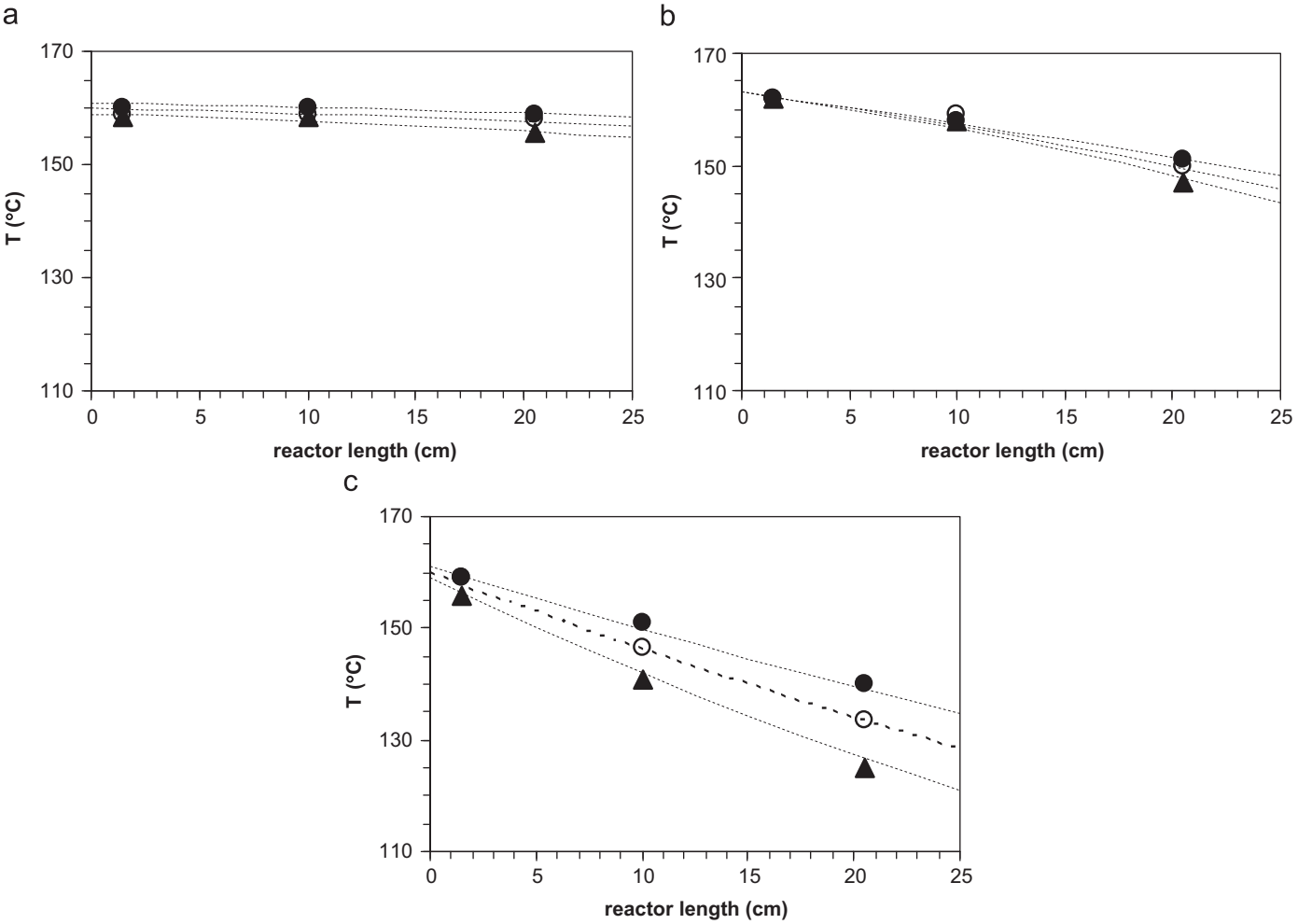

Fig. 4. Axial T profiles for different liquid flow rates and pressures; F_G=9 N L/h (carbon, rock wool foam); (a) P_T=9 bar, (b) P_T=15 bar, (c) P_T=25 bar; (●) F_L=100 ml/h, (○) F_L=60 ml/h, (▲) F_L=30 ml/h; lines represent model predictions.

are very small (see Fig. 4) and condensation of water vapor is not important. Increasing the pressure to 15 bar considerably reduces the water vapor fraction (to ca. 40%) of the flowing gas phase, but 10 to 20 times higher temperature differences develop now in axial direction (see Fig. 4b). Hence, condensation will occur along the packed bed what may explain the curved shape of the axial temperature profile. This influence should become more visible at lower liquid flow rate as Fig. 4b suggests by the increase in curving of the profiles occurring in the transition from 60 to 30 ml/h. At 25 bar of total pressure the (condensable) water vapor fraction of the flowing gas is probably becoming then small enough (ca. 15%) to mask any effect of condensation (on the profiles) although the higher temperature gradients observed at 25 bar actually enhance condensation through a stronger decrease in the water vapor pressure. The model strongly supports the aforementioned effect of condensation on heat transfer as curving of the profiles in the model could be only achieved when accounting for the contribution of water vapor condensation to the heat balance (Eq. (1)).

4.3. Effect of operating conditions

To discuss the effect of operating variables on heat transfer, all raw axial profiles were converted to axial temperature differences (ΔT) defined as the difference between the temperatures measured at axial positions of 1.5 and 20.5 cm, respectively. Fig. 5(a)–(c) plots the so obtained ΔT data against total pressure and the gas and liquid flow rates studied.

In general, total pressure, liquid flow rate and gas flow rate all seem to affect the axial ΔT. However, the influence of parameters is found to decrease in the aforementioned order (see also Section 4.4). At lower pressures (from 9 to 12 bar) and independently of the liquid and gas flow rates applied, flat axial temperature profiles establish in the column (see small ΔTs in Fig. 5) indicating a bad heat transfer inside the bed and from the bed to the wall. A further increase in total pressure goes in hand with a strong augmentation of the axial temperature differences before the ΔTs reach a plateau at 25 bar (see Fig. 5). Incrementing the pressure at constant liquid and gas flow rate leads to gradually smaller superficial gas velocities that must provide better heat transfer conditions in the bed.

For increasing liquid flow rates, the ΔTs decrease what apparently seems contradictory as smaller ΔTs could be wrongly interpreted as a sign of worse heat transfer. The axial temperature profiles that establish in the column are the consequence of a heat input and radial heat loss balance. In case of higher liquid flow rates the heat input due to forced convection proportionally increase with the product $\rho_L c_{pL} u_L$ (neglecting the contribution of the gas phase), whereas the radial heat losses ($U4/\mathrm{DI}(T-T_{\mathrm{ext}})$) are not enhanced in the same proportions due to a smaller effect of liquid flow rate (or velocity) on the overall heat transfer coefficient U.

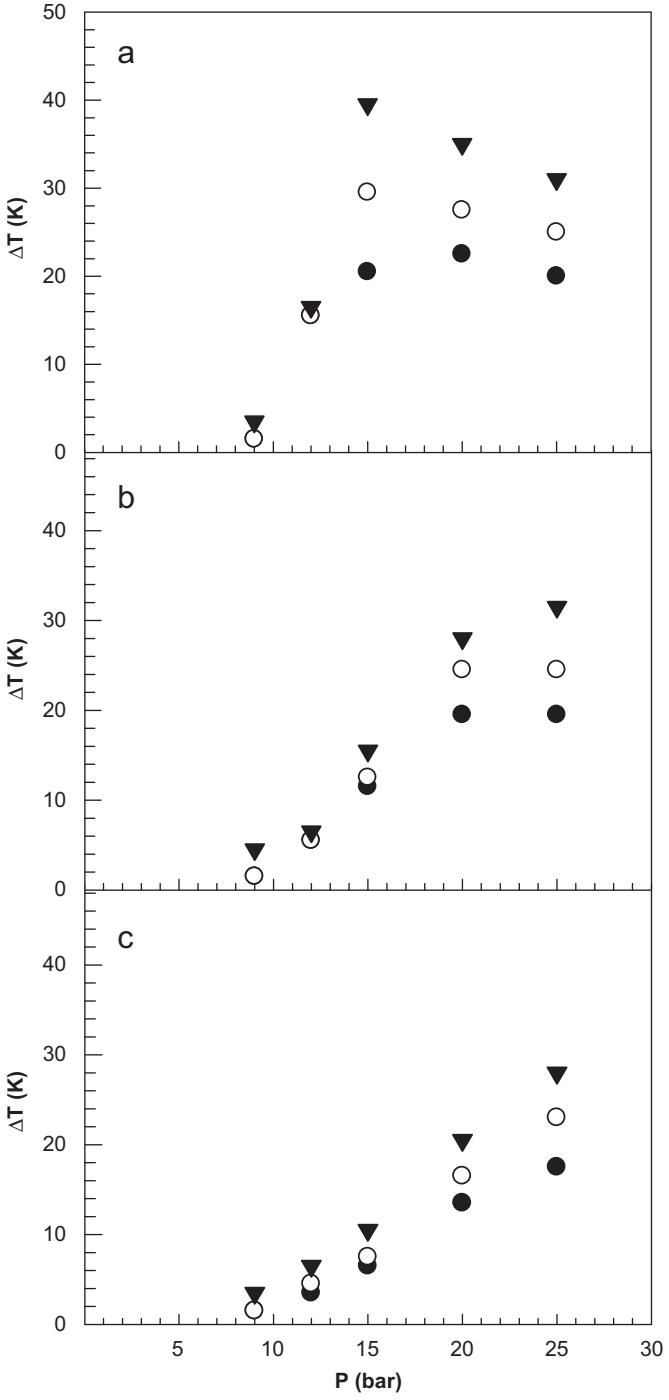

Fig. 5. Axial temperature gradient as function of system pressure for different liquid and gas flow rates; (a) F_G=3 N L/h, (b) F_G=9 N L/h, (c) F_G=18 N L/h. Symbols: (●) F_L=100 ml/h, (○) F_L=60 ml/h, (▲)F_L=30 ml/h.

4.4. Overall heat transfer coefficient U

The results of U obtained by fitting the model predictions to the experimental data are plotted in Figs. 6 and 7 for all experimental conditions studied. Both figures clearly reflect the influence of the operating parameters on heat transfer as previously established in Section 4.3. The effect of the gas flow rate on heat transfer (U) is not very relevant (see Fig. 7) for trickle flow regime (Lamine et al., 1996; Mariani et al., 2001). It is noteworthy that the study of Mariani et al. (2001) was conducted for trickle beds with: $\mathrm{DI}/d_p > 4.7$ at $5.4 < \mathrm{Re}_L < 119.6$ and $2 < \mathrm{Re}_G < 158.5$. The conditions of our work coincides in the aspect ratio, but our liquid and gas Reynolds numbers are outside at the inferior limit of the validity ranges of Mariani et al. works.

A positive effect of liquid flow rate on heat transfer is deduced from Fig. 6. Its dependency on the liquid Reynolds number is ca. 0.3 (see exponent of Re_L in correlation of h_W in Section 4.5). This generally agrees with the findings of other authors (Lamine et al., 1996; Mariani et al., 2001). The trend in these works is that the dependency (of Nu_W or Nu_T) on the liquid Reynolds number decreases with decreasing liquid and gas Reynolds number. Mariani et al. (2001) report an exponent of 0.65 of Re_L

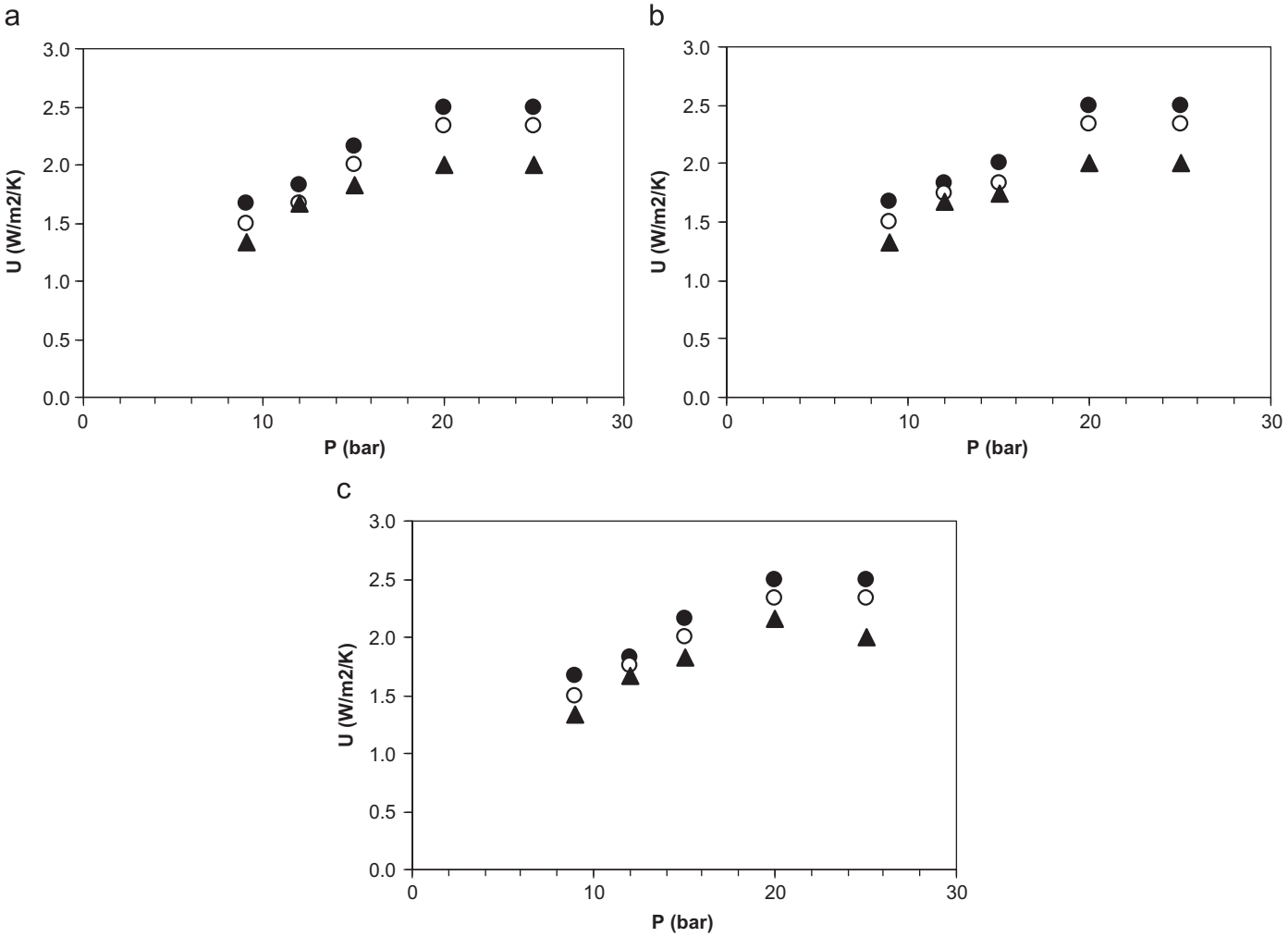

Fig. 6. Overall heat transfer coefficient as a function of system pressure; (a) F_G=3 N L/h, (b) F_G=9 N L/h, (c) F_G=18 N L/h. Symbols: (●) F_L=100 ml/h, (○) F_L=60 ml/h, (▲) F_L=30 ml/h.

for their conditions, whereas Sokolov and Yablokova (1983) (as cited in Table 2 in Lamine et al., 1996) obtained a smaller $Re_L^{0.43}$ dependency of Nu_W for the following conditions: $DI/d_p > 54$–93 at $0.2 < Re_L < 60$ and $0 < Re_G < 43$.

The strongest effect on heat transfer exerts the system pressure. From 9 to 20 bar the overall heat transfer coefficient is a quasi-linear function of pressure before becoming independent of pressure at 25 bar (see Figs. 6 and 7). This finding is interesting, but cannot be contrasted with other data due to the lack of studies that deal with the effect of pressure on heat transfer. Increasing pressure can enhance the heat transfer indirectly (since it seems to be independent on Re_G) if the related decrease in gas velocity leads to a higher liquid hold up. However, this effect alone cannot explain the strong influence of pressure observed in our study. For our particular nitrogen–water system and high temperatures, condensation of water vapor from the gas phase was identified to have a positive role on heat transfer. One can speculate that condensation may lead to the formation of a thin slowly moving liquid water layer in the column, thereby enhancing the heat transfer.

Finally, the precision of the fitted overall heat transfer coefficients has to be analyzed. The uncertainty in the fitting procedure is caused by the precision of the temperature measurement (± 0.5) and the quality of the fit particularly in case of curved profiles. All thermocouples used were calibrated against ambient and boiling water to determine and eliminate eventual differences due to the manufacturing. At the lowest system pressure of 9 bar the axial temperature differences recorded during
the experiments ranged between 2 and 5 K depending on the liquid flow rates. Assuming a maximum possible error in the ΔT measurements of 1 K, uncertainties of 20–50% in the worst case could be propagated to the fitting of U by Eq. (1). For higher system pressures, the ΔTs measured sharply increased and at 15 bar the maximum uncertainty in U due to errors in the ΔT measurements reduces now to 2.5–10%. On the other, at intermediate system pressures of 12 and 15 bar, curved profiles occurred in particular at the lowest liquid velocity of 30 ml/h. The fit of these profiles although acceptable showed a higher deviation than that of straight profiles, which are very easy to match. The highest precision should therefore result for the values of U fitted at 20 and 25 bar. The convex curving of the temperature profiles disappeared at these pressures and the highest deviation introduced by the error of the thermocouples was between 2.5% and 5%.

4.5. Bed to wall heat transfer h_W

With the help of Eq. (4) and the fitted overall heat transfer coefficients, the bed to wall heat transfer coefficient h_W was evaluated for all experimental conditions used. Obtained values of

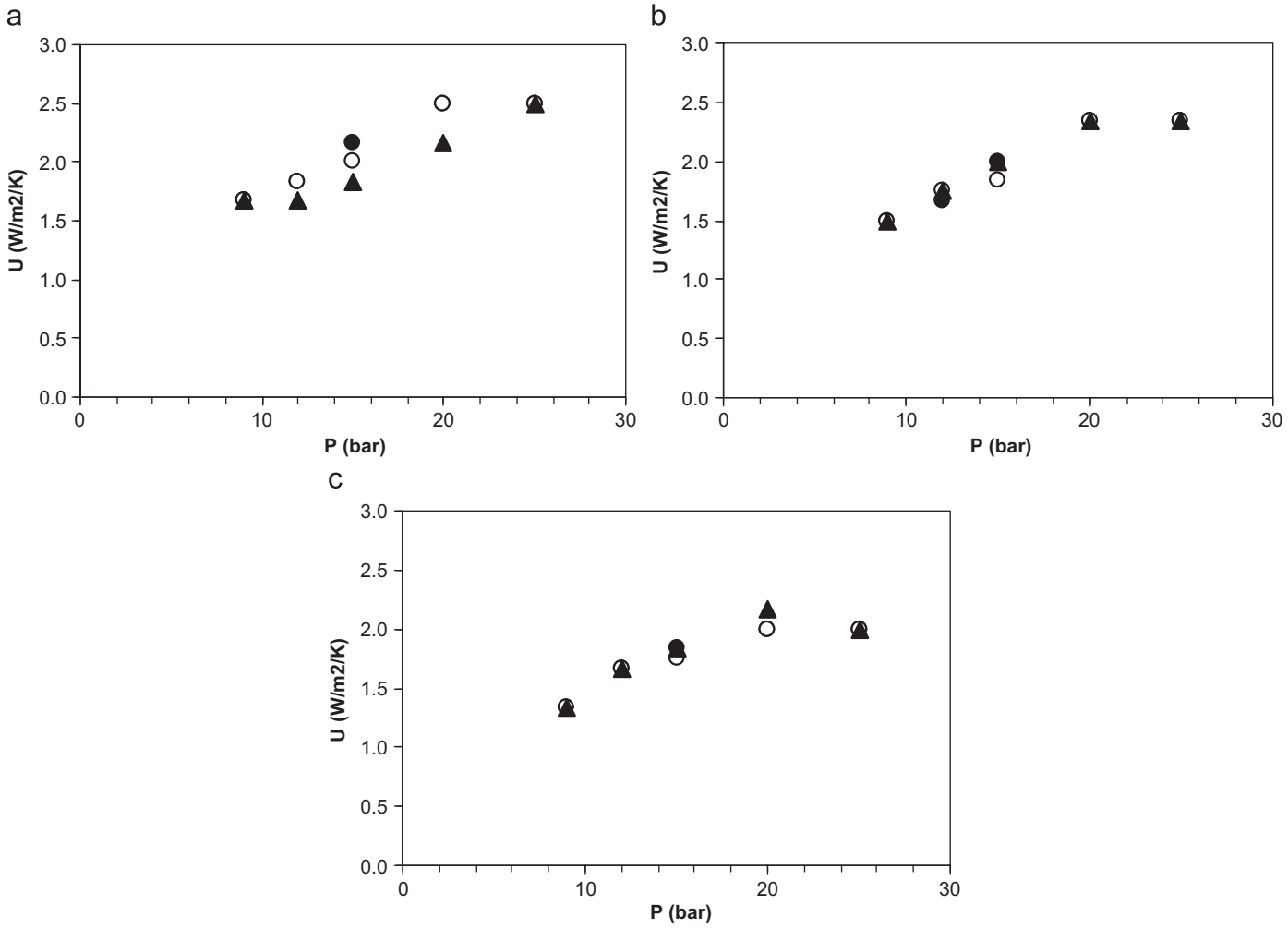

Fig. 7. Overall heat transfer coefficient as a function of system pressure; (a) F_L=100 ml/h, (b) F_L=60 ml/h, (c) F_L=30 ml/h. Symbols: (●) F_G=18 N L/h, (○) F_G=9 N L/h, (▲) F_G=3 N L/h.

h_W vary between 2 and 8 W/(m^2 K), hence being close but always superior to the coefficients of h_W calculated with the correlation proposed by Specchia et al. (1980) for the limiting case of gas–solid heat transfer. This result may not surprise since the liquid flow rates used in our work are very small and conditions that arise for bed to wall heat transfer could be quite similar to those of a gas–solid system. The precision of the h_W coefficients not only depends on the quality of the fitting of U, but also on to what extent the bed to wall heat transfer is the controlling resistance of the process. For our system, the corresponding thermal resistances of the natural convection, heat conduction in the insulating material and bed to wall heat transfer are calculated to 0.027, 0.22 and 0.125–0.5 m^2 K/W. As expected, natural convection outside the insulating material is not controlling its resistance typically being ten times smaller than the other two resistances. Accordingly, both the bed to wall heat transfer and the insulating heat conduction are controlling steps in the overall heat transfer. For pressures up to 15 bar, h_W exerts a stronger control than heat conduction, but then the resistances become similar. This means that the uncertainty in h_W is a function of its absolute value being smaller for low h_W. Overall, h_W is found to exactly follow the trends as observed for U providing thus confidence to the estimated values of h_W.

The values of h_W were correlated with operating conditions employing the following expression assuming the usual Chilton–Coburn dependency for the Prandtl number:

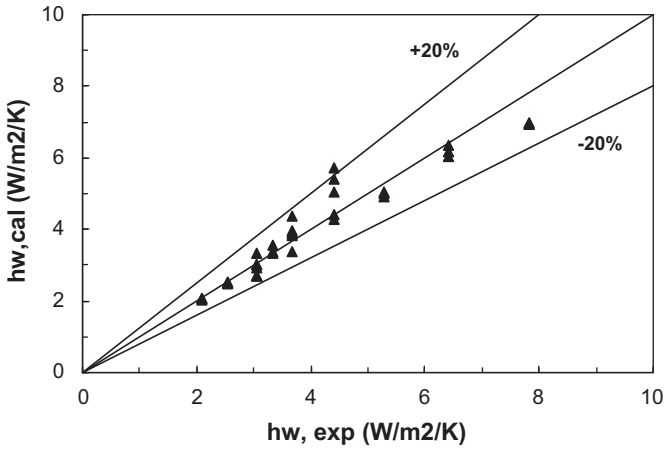

Fig. 8. Parity plot for experimentally determined h_W and values calculated from the correlation proposed in Eq. (5).

$$h_W = 0.1738\,\mathrm{Re}_L'^{0.305}\mathrm{Pr}_L^{1/3}\mathrm{Re}_G'^{0.0475}P_T^{0.98} \quad (5)$$

for DI/d_p=18.6, $0.16 < \mathrm{Re}'_L < 1.0$, $0.35 < \mathrm{Re}'_G < 4.5$ and 9 bar $< P_T <$ 20 bar.

The optimized exponents for the gas and liquid Reynolds number and total pressure clearly reflects the experimental trends outlined in the previous sections. The calculated average error of the correlation proposed is small (ca. 7%) with 12 data points with a negative deviation and 24 data points with a positive deviation. The overall quality of the fit can be appreciated in Fig. 8, which shows a parity plot of experimentally determined h_W values and h_W values predicted by the correlation of Eq. (5). It can be concluded that the correlation suitably represents the experimental data, although its use is restricted to a narrow range of operating conditions that includes a variation of the system pressure.

4.6. Feed temperature modulation without reaction

The results of experiments conducted with imposed temperature feed modulation are illustrated in Fig. 9 for a total pressure of 15 bar a gas flow rate of 9 N L/h and three different liquid low rates. The cycle period and split for these experiments were set to respectively 108 min and 5/6, i.e. feed temperature was periodically modulated between 25 °C during 18 min to 159 °C during 90 min. However, the arrangement of the tubing and inlet column connections originates a distortion of the ideal square wave for the feed temperature and generates a V-shaped temperature distribution at the column inlet similar to the measured profiles at $z=1.5$ cm (see Fig. 9). In all cases, the liquid flow rate is not high enough to cool the hot reactor inlet to ambient temperature within 18 min. A longer time interval with cold flow would be needed, i.e. a smaller split or a higher cycle period, to achieve this goal. When switching back to hot feed flow, the temperature raises faster to reach a pseudo-steady state at 159 °C. Thus, a temperature wave establishes in the reactor inlet and propagates downstream to the column exit. The speed of traveling waves increases with the liquid holdup and therefore with increasing liquid flow rate.

Simulated profiles using the values of U evaluated in Section 4.4 are also plotted in Fig. 9. The model predicts very well all experimental profiles close to the inlet zone, although a slight but progressive deviation is observed in the simulations of the temperatures towards the column outlet. The dynamics of heat transfer predicted by the model is slightly slower than the one exhibited by the experimental data. Parametric analysis (not shown here) allowed identifying the relevance of the liquid holdup as a key parameter that defines the temperature wave velocity along the bed. This highlights the need of an accurate estimation of liquid holdup to succeed in modeling non-steady state operation of trickle bed reactors. Moreover, the thermal dynamics of the insulated column, which is not considered in the model formulation, could influence the temperature profiles inside the bed and partly be responsible for the deviation observed.

5. Conclusions

Steady state axial temperature profiles have been measured in a rock wool insulated packed bed column with co-current

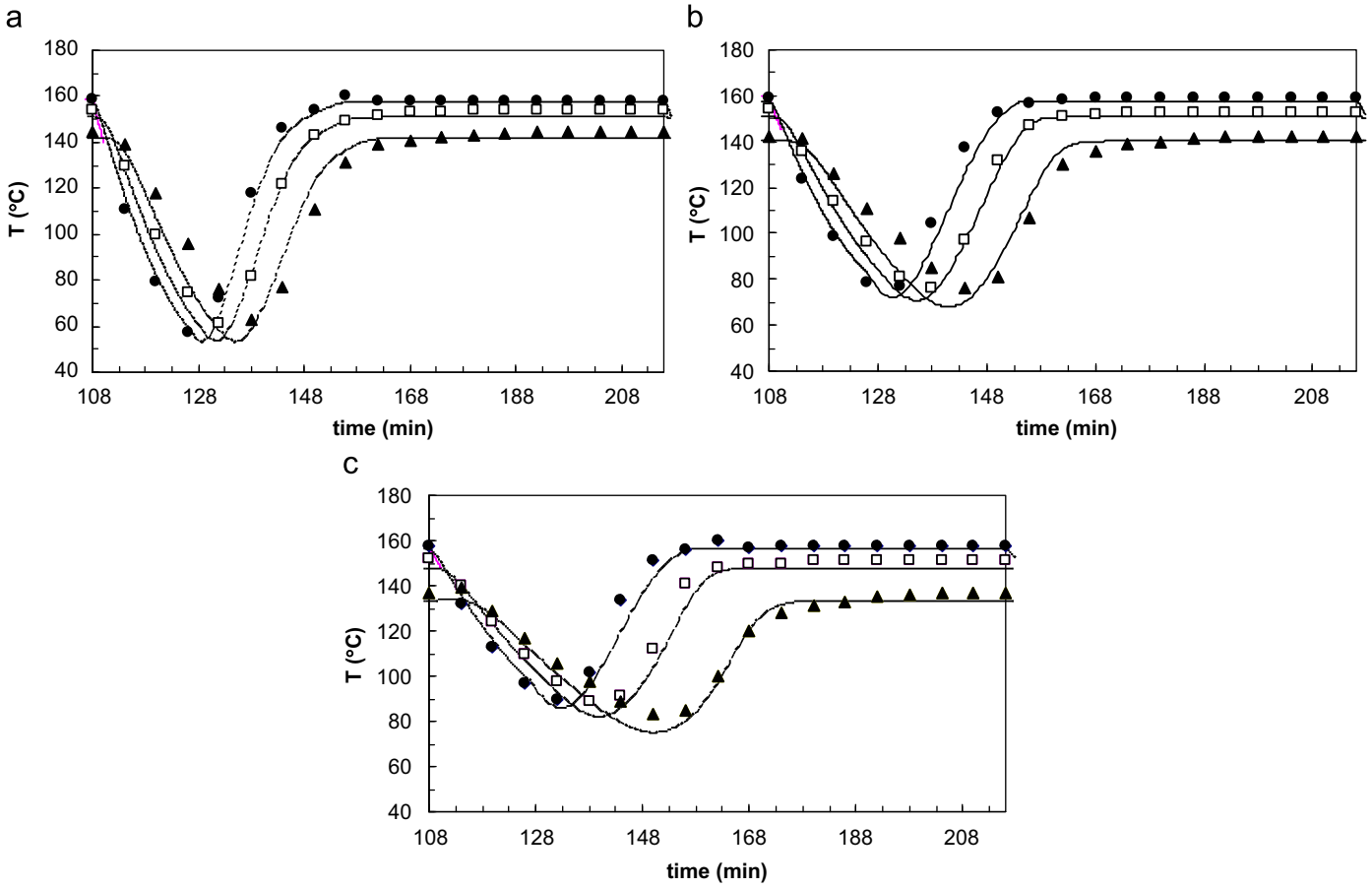

Fig. 9. Evolution of axial temperatures during operation with imposed feed temperature modulation: $P_T=15$ bar, $F_G=9$ N L/h, period = 1.8 h, split = 5/6, (a) $F_L=100$ ml/h, (b) $F_L=60$ ml/h, (c) $F_L=30$ ml/h, Rock wool foam. Symbols: (●) T (1.5 cm), (□) T (10 cm), (▲) T (20.5 cm); discontinuous lines represent model predictions.

downflow of nitrogen and water phases for different column pressures and very small gas and liquid flow rates corresponding to the low interaction regime.

The experimental results confirm the trends reported in literature that the gas flow rate only marginally affects the heat transfer, whereas increasing the liquid flow rate enhances the heat transfer from the bed to wall. However, a linear pressure dependency of heat transfer is observed from 9 to 20 bar before it levels off at 25 bar. At intermediate pressures, convex curving of the profiles occurred suggesting that condensation of water vapor from the gas phase impact on the heat transfer conditions inside the packed bed.

The whole data set was interpreted with a pseudo-homogeneous one parameter model confirming the influence of condensation of water vapor on heat transfer. Curving of the profiles as observed in the experiments could be only reproduced by the model when accounting for the contribution of condensation to the heat balance.

Overall heat transfer coefficients U based on the inside column area were evaluated by fitting the model predictions to the experimental data. The values of U obtained (1.25–2.5 W/m^2 K) quantitatively reflect the aforementioned influences of operating variables on heat transfer. The uncertainty in U is pressure dependent because at low system pressure the bed gradients are small and the error of the thermocouples can become important (only at 9 bar). Curving of the profiles (essentially occurring at pressures of 15 bar) is a second contribution that can moderately increase the uncertainty since fitting of curved profiles is acceptable but not as precise as fitting of straight profiles.

Bed to wall heat transfer coefficients (h_W) were inferred from the values of U (Eq. (4)) and accurately correlated with operating conditions by the following expression:

$$h_W = 0.1738\,\mathrm{Re}'^{0.305}_L\,\mathrm{Pr}_L^{1/3}\,\mathrm{Re}'^{0.0475}_G\,P_T^{0.98}$$

for $\mathrm{DI}/d_p = 18.6$, $0.16 < \mathrm{Re}'_L < 1.0$, $0.35 < Re'_G < 4.5$ and 9 bar $< P_T <$ 20 bar.

In agreement with the very small liquid flow rates employed in the experiments, the values of h_W (between 2 and 8 W/m^2 K) are close to those for the limiting case of gas–solid heat transfer. The average error in h_W calculated from the correlation is less than 7%. As in our work the use of an insulating material is mandatory, a mixed control of heat transfer results, although the bed to wall heat transfer is the larger resistance at least for pressures up to 15 bar. Overall however, it can be concluded that the correlation suitably represents the experimental data.

The experiments conducted with imposed temperature feed modulation reveal the formation of V-shaped temperature profiles (due to the experimental arrangement of tubing and column inlet connections) and a certain expansion while propagating through the packed column. The accurate modeling of these temperature waves was achieved with the dynamic model using the previously fitted values of U. Parametric analysis indicated that the dynamics of heat transfer is particularly sensitive to the value of the dynamic liquid hold up. The overall performance of the model developed (including the fitting of U) gives confidence for its ultimate application in the investigation of the catalytic wet air oxidation of phenol over active carbon conducted in a trickle bed reactor under temperature feed modulation.

Nomenclature

c_p	specific heat (kJ/mol K)
DI	internal diameter of reactor (m)
d_p	particle diameter (mm)
F	fluid flow rate (ml/h or N L/h)
h	heat transfer coefficient (W/m^2 K)
k	thermal conductivity (W/m K)
L	reactor length (cm or m)
P	total pressure (atm or bar)
R	column radius (m)
Re	Reynolds number ($\rho u d_p/\mu$)
Re′	Reynolds number ($\rho u d_p/\mu\varepsilon$)
T	temperature (K or °C)
t	time (h)
u	superficial velocity (m/h)
U	overall heat transfer coefficient (W/m^2 K)
z	axial bed position (cm or m)

Greek letters

ΔH^V	evaporation enthalpy (kJ/mol)
α	molar flow rate (mol/h)
ε	phase hold up ($m^3_{phase}/m^3_{reactor}$)
ε_p	particle voidage ($m^3_{particle\ void}/m^3_{rparticle}$)
ε_B	bed voidage ($m^3_{void}/m^3_{reactor}$)
ρ	density (g/m^3)
μ	dynamic viscosity (g/m h)

Superscripts and subscripts

0	initial value
1	inner column radius
2	outer column radius
B	bed
G	gas
IN	insulation
L	liquid
NAT	natural convection
R	reactor
s	solid
T	total
v	vapor
w	water
W	bed to wall

Acknowledgments

This work was funded by AECID, Projects A/4887/06, A/9419/07 y A/017018/08 and the authors are grateful to CONICET and UNMdP for their financial support. Further fund contribution was possible by the European Commission through REMOVALS Project FP6-018525. The researchers from the Rovira i Virgili University are also supported by the Comissionat per a Universitats i Recerca del DIUE de la Generalitat de Catalunya (2009 SGR 865). Finally, the authors would like to thank Prof. Osvaldo Martinez for his valuable comments.

References

Babu, B.V., Sastry, K.K.N., 1999. Estimation of heat transfer parameters in a trickle bed reactor using different evolution and orthogonal collocation. Computers and Chemical Engineering 23, 327–339.

Churchill, S.W., Chu, H.H.S., 1975. Correlating equations for laminar and turbulent free convection from a vertical plate. International Journal of Heat and Mass Transfer 18, 1323–1329.

Dudukovic, M.P., Larachi, F., Mills, P.L., 2002. Multiphase catalytic reactors: a perspective on current knowledge and future trends. Catalysis Reviews: Science and Engineering 44, 123–246.

Gabbiye, N., Stüber, F., Font, J., Bengoa, C., Fortuny, A., Fabregat, A., Haure, P., Ayude, A., 2009. Feed temperature modulation in trickle bed reactor: experiments and modelling. In: Proceedings of the Eighth World Congress of Chemical Engineering, Montréal, Quebec, Canadá.

Khadilkhar, M.R., Mills, P.L., Dudukovic, M.P., 1999. Trickle bed reactor models for systems with a volatile liquid phase. Chemical Engineering Science 54, 2421–2431.

Lamine, S., Gerth, L., Le Gall, H., Wild, G., 1996. Heat transfer in a packed bed reactor with cocurrent downflow of a gas and a liquid. Chemical Engineering Science 51, 3813–3827.

Lange, R., Schubert, M., Bauer, T., 2005. Liquid holdup in trickle-bed reactors at very low liquid Reynolds numbers. Industrial and Engineering Chemistry Research 44, 6504–6508.

Mariani, N.J., Martínez, O.M., Barreto, G.F., 2001. Evaluation of heat transfer parameters in packed beds with cocurrent downflow of liquid and gas. Chemical Engineering Science 56, 5995–6001.

Mears, D.E., 1971. Industrial and Engineering Chemistry Process Design and Development 10, 541.

Mederos, F.S., Ancheyta, J., Chen, J., 2009. Review on criteria to ensure ideal behaviors in trickle-bed reactors. Applied Catalysis A: General 355, 1–19.

Silveston, P.L., Hanika, J., 2002. Challenges for the periodic operation of trickle-bed catalytic reactors. Chemical Engineering Science 57, 3373–3385.

Sokolov, V.N., Yablokova, M.A., 1983. Thermal conductivity of a stationary granular bed with upward gas–liquid flow. Journal of Applied Chemistry of the USSR 56, 551–553.

Specchia, V., Baldi, G., Sicardi, S., 1980. Heat transfer in packed bed reactors with one phase flow. Chemical Engineering Communications 4, 361–380.